

Supplementary information of

Exploring the boundaries in the analysis of large particles by single particle inductively coupled plasma mass spectrometry: Application to nanoclays

David Ojeda, Eduardo Bolea, Josefina Pérez-Arantegui, Francisco Laborda

Group of Analytical Spectroscopy and Sensors (GEAS)

Institute of Environmental Sciences (IUCA)

University of Zaragoza

Pedro Cerbuna 12, 50009 Zaragoza, Spain.

Index

S1. Isolation of particles below 1 μm from kaolin suspension by centrifugation

S2. Digestion of samples containing nanoclays for total Al analysis by ICP-MS

S3. Determination of limits of detection in terms of size and number concentration in SP-ICP-MS

S4. Calculations for the determination of the upper size limit measurable by SP-ICP-MS

S5. Ionisation efficiency for SiO_2 particles

S6. Analysis of Al_2O_3 particles by SP-ICP-MS using ^{27}Al

S7. Determination of thickness for kaolinite particles in TEM images

S8. Migrated particles from material #1 observed by TEM

S1. Isolation of particles below 1 μm from kaolin suspension by centrifugation

To isolate the fraction below 1 μm , the original product was suspended in ultrapure water at a starting concentration of 1000 mg L^{-1} of kaolin. After 1 hour of decantation, 15 mL of the supernatant were withdrawn from the suspension and finally centrifuged during 5 min at 1200 rpm. These conditions are the result of the calculations made considering the particles characterised were kaolinite ($\text{Al}_2\text{Si}_2\text{O}_5(\text{OH}_4)$), which is the main crystalline structure of the sample according to their analysis by X-ray diffraction, with a particle density of 2.6 g cm^{-3} . The mass fractions regarded for Al and Si are 18.0 and 21.7, respectively, determined from their molar fraction.

S2. Digestion of samples containing nanoclays for total Al analysis by ICP-MS

The procedure described by Inorganic Ventures for the elemental analysis of Zeolites was followed (<https://www.inorganicventures.com/guides-and-papers/elemental-analysis-of-zeolites>). It is based on the use of two reagents: UA-1 and UNS-1 (Inorganic Ventures, Christiansburg, USA). The first one is an acid reagent composed by HCl 20% (v/v) and HF 80% (v/v), whereas UNS-1 is a neutralising and a stabilising reagent which contains Triethylenetetramine (10-25% (v/v)). In this procedure the use of boric acid to eliminate the HF added in excess is unnecessary since pH conditions allow working with the fluorides mostly unprotonated. The procedure consists of the following steps, adapted to the sample conditions treated in this work:

1. A specific mass from the sample is weighed in a low density polyethylene bottle (LDPE) of 250 mL. Depending on the sample, the amount of mass is:

—For kaolin, 50 mg of original powder.

—For the fraction of particles below 1 μm of size from kaolin, 1 mL of suspension (supernatant after centrifugation).

—For the solutions from migration tests, either the material #1 or #2, 5 mL of volume.

2. In the case of solid samples, 10 drops of ultrapure water are added to the sample and then softly stirred, so the sample remains hydrated and not agglomerated.

3. 5 mL of reagent UA-1 and 0.25 mL of HNO_3 70% (v/v) J.T. Baker are added. The bottle is closed and it is shaken for over 2 minutes.

4. 25 mL of UNS-1 are added. The final weight is adjusted until 100 g with the addition of ultrapure water. The final solution is mixed by inverting it manually at least 50 times.

S3. Determination of limits of detection in terms of size and number concentration in SP-ICP-MS

Limits of detection (both in size and in number concentration) for the analysis by SP-ICP-MS in different conditions were calculated following the expressions:

$$LOD_{size} = X_C^{size} = \left(\frac{15\sigma_B}{\frac{1}{w_p} \pi \rho F_p K_{ICP-MS} K_M t_{dwell}} \right)^{1/3} \quad (\text{Eq. 2})$$

$$LOD_{number} = \frac{5\sqrt{Y_{N,B}} + 3}{\eta Q_{sample} t_i} \quad (\text{Eq. 3})$$

where σ_B is the standard deviation of the baseline of a blank, w_p the time-width for a transient particle event (in terms of time), ρ is the density, F_p is the mass fraction of the element in the particle, t_{dwell} is the dwell time, K_{ICP-MS} is the factor referred to the detection efficiency of the system, in which it is represented the ratio of the number of ions detected

vs. the number of analyte atoms of the measured isotope into the ICP. $K_M (=AN_{Av}/M_M)$ is a factor related to the element measured, where A is the atomic abundance of the isotope considered, N_{Av} the Avogadro number, and M_M the atomic mass of the element. On the other hand, $Y_{N,B}$ is the number of events detected in the blank, η the transport efficiency, Q_{sample} is the sample introduction flow and t_i the acquisition time.

S4. Calculations for the determination of the upper size limit measurable by SP-ICP-MS

In the analysis of both SiO_2 and kaolinite particles (Sections 3.1 and 3.3, respectively) limitations related to the detector signal in pulse mode were observed for large particles. To estimate a limit above which the detector response would be affected, several profiles from the peaks detected by SP-ICP-MS during a measurement were studied. In the case of SiO_2 particles, using the isotope ^{29}Si , the maximum signal intensity was observed at 1560 counts (Figure S1a) for a dwell time of 100 μs .

Figure S1

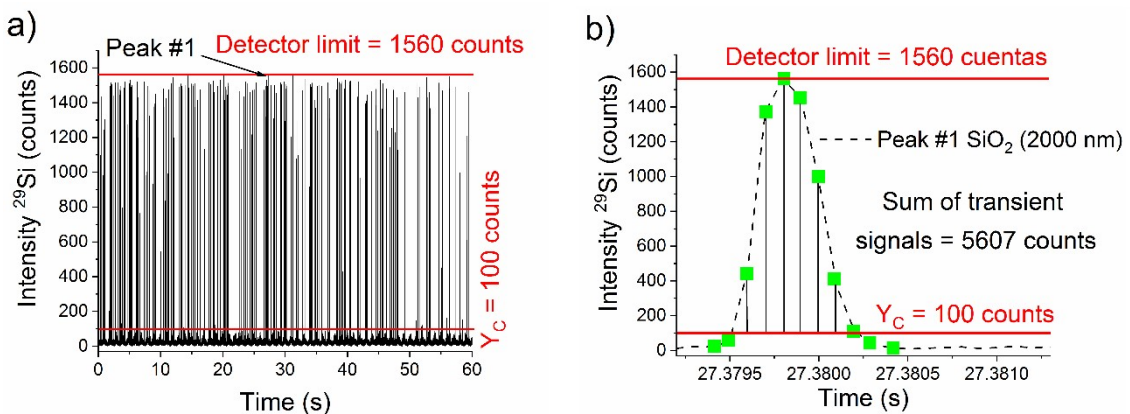


Figure S1. a) Time scan for size standard of 2000 nm of SiO₂ particles for the study of the upper size limit, determined at 1560 counts. b) Profile of a single peak detected at the maximum intensity. Transient signals for the peak are displayed as green dots.

Some peaks for the size standard of 2000 nm (nominal diameter) were confirmed to be uncompleted at this level, as can be seen in Figure S1b, whose profile is flattened at the top, losing some information in terms of intensity and, therefore, in terms of mass and size. Considering a width of 800 μ s (the average value for the largest peaks detected with a complete profile), a symmetrical peak was modelled reaching the intensity of 1560 counts (Figure S2). Integrating its corresponding signal (sum of the transient signals) and transforming it into size, it was determined that the upper size limit (as equivalent diameter of a SiO₂ particle) was of 1200 nm, which means that below this size the characterisation would be correct under the conditions studied.

Figure S2

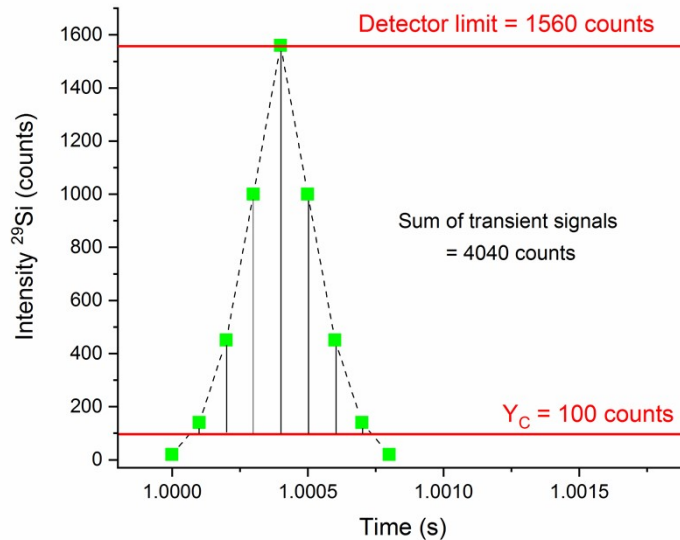


Figure S2. Modelled peak for the size determination above which the characterisation of SiO₂ particles will be affected by limitations related to the detector, established in 1560 counts. Transient signals for the peak are displayed as green dots.

For the kaolin, using the isotope ^{27}Al during the analysis, a maximum in the signal intensity was observed at 1625 counts (Figure S3). In a similar way, the modelled peak allowed to determine the upper size limit at 420 nm of equivalent diameter for kaolinite particles (Figure S4).

Figure S3

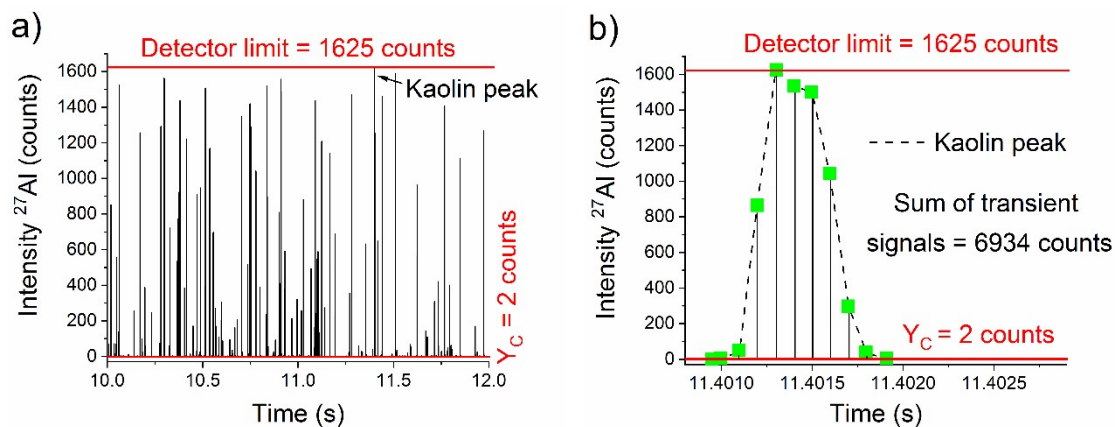


Figure S3. a) Time scan for the fraction of particles below $1\ \mu\text{m}$ from kaolin. b) Profile of a single peak detected at the maximum intensity for the study of the upper size limit, determined at 1625 counts. Transient signals for the peak are displayed as green dots.

Figure S4

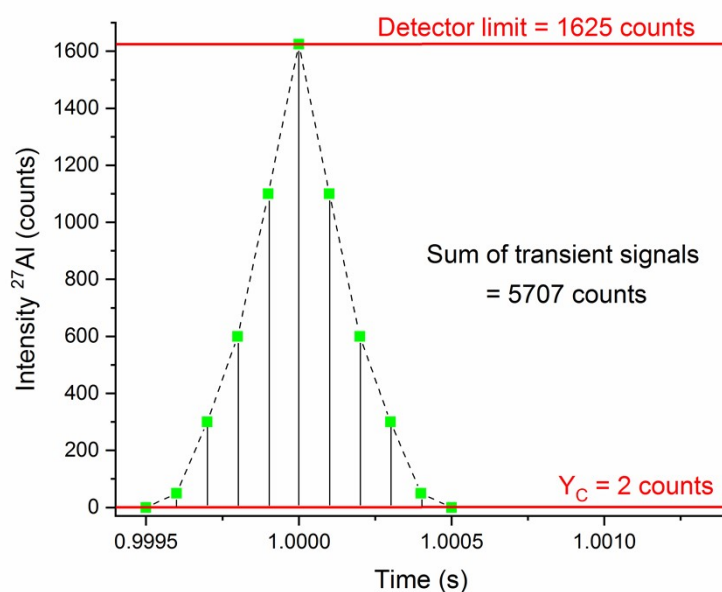


Figure S4. Modelled peak for the size determination above which the characterisation of kaolinite particles will be affected by limitations related to the detector, established in 1625 counts. Transient signals for the peak are displayed as green dots.

S5. Ionisation efficiency for SiO₂ particles

The mean intensity from peaks detected were plotted vs. the nominal size for different SiO₂ standards (500, 1000 and 2000 nm) to study their ionisation efficiencies (Figure S5). Given the linear relationship between the logarithms of these two parameters, a theoretical slope of 3 would be expected if ionisation of the particles were complete.

Figure S5

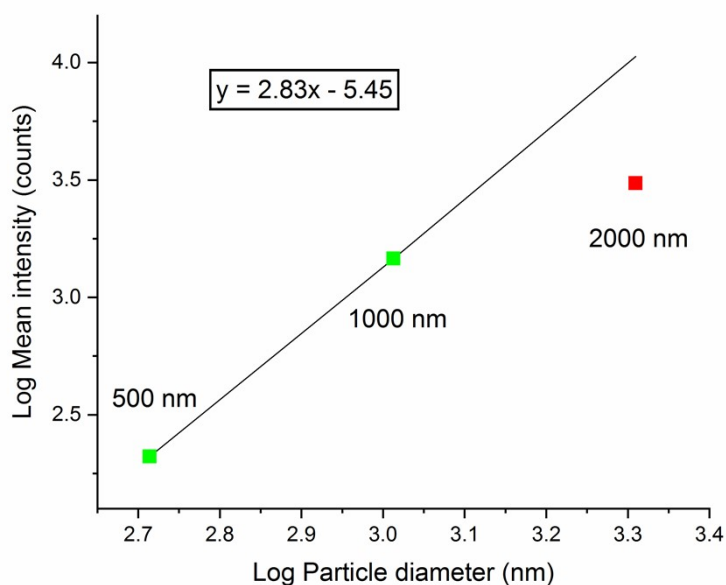


Figure S5. Logarithm of the mean intensity obtained plotted vs. the logarithm of the nominal particle diameter for SiO₂ size standards of 500, 1000 and 2000 nm.

S6. Analysis of Al₂O₃ particles by SP-ICP-MS using ²⁷Al

The method developed was applied to a commercial suspension of Al₂O₃ particles ranging from nominal size of 30 to 60 nm. Size distribution is shown in Figure S6, in accordance to the values specified by the manufacturer, and values of 40 nm as the most frequent size.

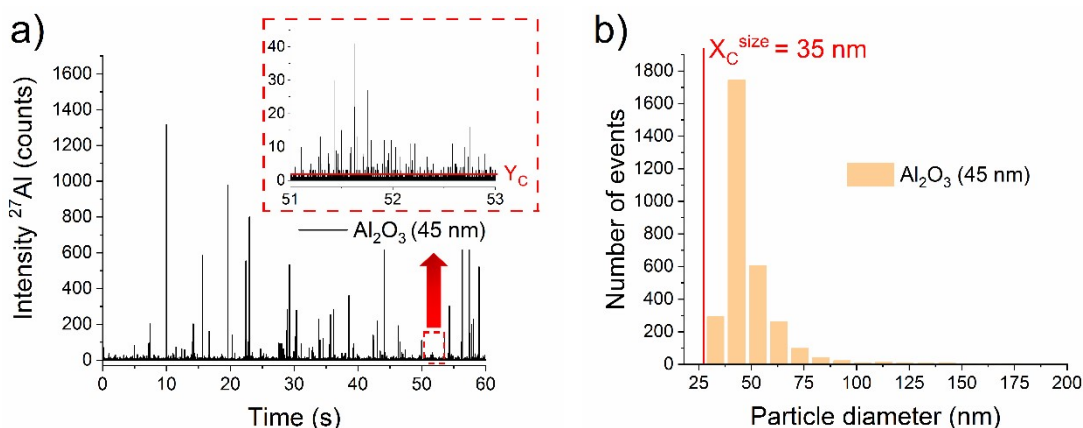
Figure S6

Figure S6. Time scan using ^{27}Al for Al_2O_3 particles from a commercial suspension (45 nm of nominal size). b) Particle size distribution obtained by SP-ICP-MS. Critical value (Y_C) applied of 2 counts, which in terms of size equals 35 nm (X_C^{size}).

The use of ^{27}Al as the isotope of analysis allowed to reduce the LOD_{size} to 35 nm in comparison to ^{29}Si . Given the proximity to the critical value (Y_C), the distribution obtained is not complete, with a nebulization efficiency of 35%, as can be seen in Table S1.

Table S1. Size characterisation of Al_2O_3 particles from a commercial suspension by SP-ICP-MS. Most frequent size shown in brackets. Results for ^{27}Al , expressed as mean \pm s ($n = 3$).

Al_2O_3 suspension*	Average peak intensity (counts)	Average diameter (nm)	N° of events	Nebulisation efficiency (%)
45 nm (30 - 60 nm)	21 ± 2	50 ± 1 (43 ± 2)	3128 ± 36	34.9 ± 0.4

* Average nominal diameter and distribution (in brackets) specified by the manufacturer, determined by TEM.

S7. Determination of thickness for kaolinite particles in TEM images

Average values of thickness were determined by EELS for the calculation of equivalent diameters of kaolinite particles shown in TEM images (Figure S7).

Figure S7

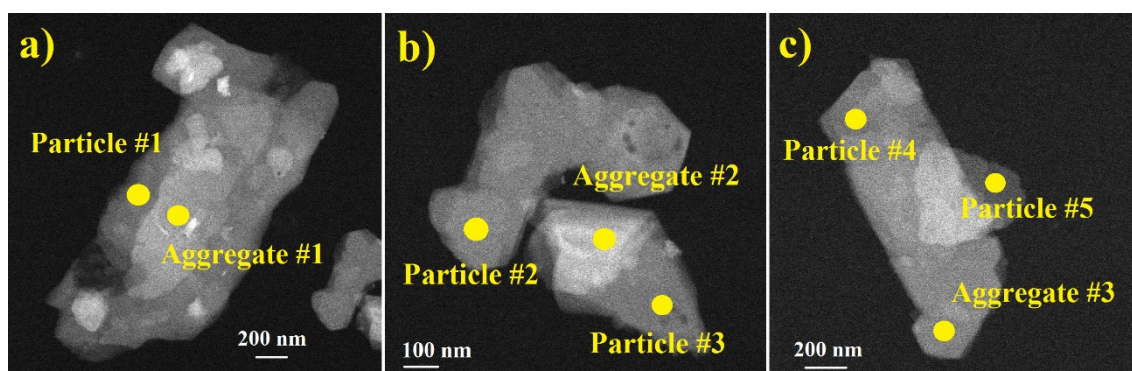


Figure S7. HAADF-TEM images of kaolinite particles (fraction below 1 μm) for the thickness determination by EELS, differentiating between individual laminates and aggregates.

Two different methods were compared: log-ratio absolute and Kramers-Kronig sum, obtaining similar results in both cases (verified by *t*-test, 95% confidence interval). Given the aggregation of particles observed by TEM, two different average thicknesses were determined: 50 nm for individual particles and 80 nm for aggregates (Table S2).

Table S2. Thickness determination for kaolinite particles by EELS with two different methods. Results shown as the average $\pm s$ ($n = 5$).

Kaolinite particles	Average thickness from two methods (nm)	
	Log-ratio absolute	Kramers-Kronig
Individual particles	56.2 \pm 6.2	53.3 \pm 2.9
Aggregates	78.6 \pm 4.3	73.2 \pm 6.1

S8. Migrated particles from material #1 observed by TEM

Particles of several micrometers were observed by TEM (Figure S8a) with high contents in carbon. Inside these particles, hexagonal structures with presence of aluminium and silicon were confirmed by EDS spectra (Figure S8b).

Figure S8

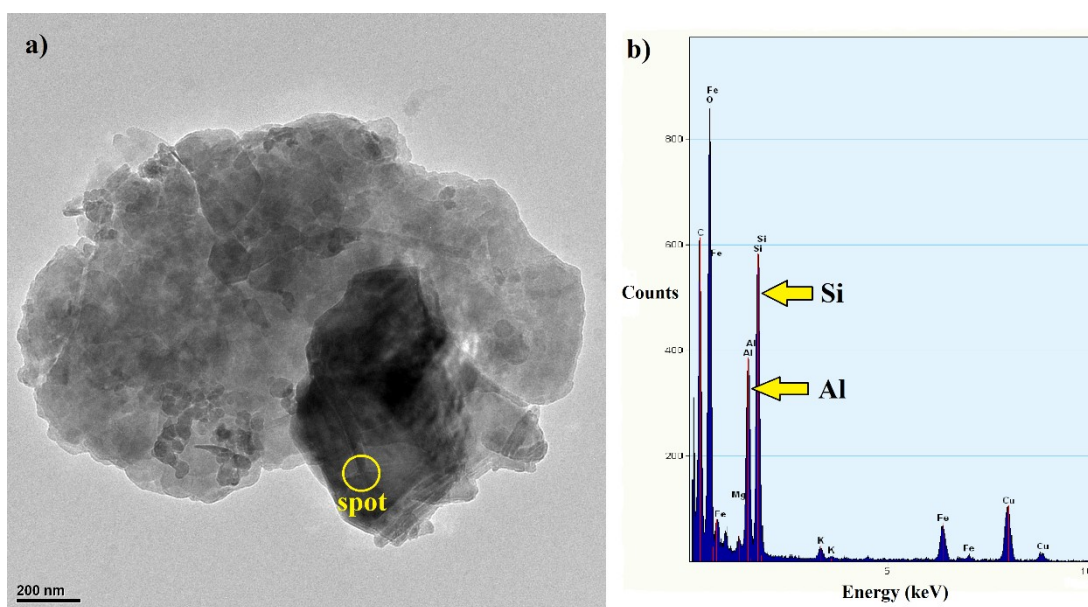


Figure S8. a) TEM image of a microfragment migrated from material #1, with hexagonal structures embedded containing Al and Si. b) EDS spectre for the spot highlighted.